Effect of surface finishing on tribological properties of ZrO_2-based composites

K. Bonny*[(1)], Y. Perez[(1)], J. Van Wittenberghe[(1)], P. De Baets[(1)], J. Vleugels[(2)], B. Lauwers[(3)]**
[(1)]Ghent University, Mechanical Construction and Production Department, Sint-Pietersnieuwstraat 41, 9000 Gent, Belgium
[(2)]Catholic University of Leuven, Metallurgy and Materials Engineering Department, Kasteelpark Arenberg 44, 3001 Leuven, Belgium
[(3)]Catholic University of Leuven, Mechanical Engineering Department, Celestijnenlaan 300 B, 3001 Leuven, Belgium
***Corresponding author: koenraad.bonny@UGent.be / koenraad.bonny@gmail.com**
**** Presenting author: yeczain.perez@UGent.be**

Abstract: Laboratory-made ZrO_2-based composites with 40 vol. % WC, TiCN or TiN were tested in dry sliding contact with WC-6wt%Co cemented carbide using an ASTM G133 pin-on-flat configuration. Surface characterization included profilometric measurement, scanning electron microscopy, energy disperse X-ray analysis and X-ray diffraction. ZrO_2-based composites with wire-EDM surface finish displayed higher friction coefficient and wear level compared to their ground equivalents. This finding was correlated to flexural strength measurements, revealing strong discrepancy between both surface finishes. ZrO_2-WC composites exhibited superior tribological characteristics compared to the ZrO_2-TiCN and ZrO_2-TiN grades.

Key words: ZrO_2-based composite, wire-EDM, dry reciprocating sliding wear

1. INTRODUCTION

Stabilized and toughened zirconia (ZrO_2) ceramics are reported to show high potential for various wear applications [1,2]. Recent developments are focused on the incorporation of secondary phases [3] such as WC [4], $TiC_{0.5}N_{0.5}$ [5] or TiN [6] into a ZrO_2 matrix. These reinforcements not only improve hardness [7] but also reduce electrical resistivity, making the ZrO_2 composites feasible for electrical discharge machining (EDM) [8]. Unlike traditional cutting and grinding processes which rely on much harder tools or abrasives to remove the softer work-material, EDM uses a series of discrete electrical sparks to erode the superfluous work-material and to generate the desired shape. However, difficulties also arise with respect to the control of surface finish [9,10] or friction and wear characteristics [10-12]. Therefore, detailed information on the impact of EDM on tribological properties of ZrO_2-based composites is crucial to improve the performance reliability associated with the structural application of EDM'ed ZrO_2-based composites. This paper focuses on hot pressed yttria-stabilised ZrO_2-based composites with 40 vol.% TiN, TiCN or WC. Friction and wear properties were examined in relation to secondary phases and surface finish variants corresponding to wire-EDM or abrasive grinding.

2. EXPERIMENTAL PROCEDURE

The zirconia-based composites were obtained by hot pressing yttria-stabilised ZrO_2 powder mixtures with 40 vol.% WC, $TiC_{0.5}N_{0.5}$ or TiN. More information on processing and characterisation is given elsewhere [4-6]. Mechanical and physical properties as well as results of grain size measurements of the secondary phase of the ZrO_2-WC, ZrO_2-TiCN and ZrO_2-TiN grades are listed in Table 1. The reported values are averages of 5 measurements.

Table 1: Physical and mechanical properties and grain size distribution for ZrO_2-based composites

Grade	A	B	C	D	E
Secondary phase and crystal size[a] [nm]	WC (20-40)	WC (800-1000)	TiCN (1600)	TiCN (<100)	TiN (800-1200)
E [GPa]	328±2	340±6	284±2	307±2	274±1
HV_{10} [kg/mm^2]	1691±8	1502±9	1422±10	1629±8	1370±7
$K_{IC,10kg}$ [MPa.m$^{1/2}$]	8.5±0.4	8.5±0.2	7.0 ± 0.2	3.9±0.1	5.6 ± 0.1
Density [g/cm^3]	9.80	9.79	5.76	5.59	5.81
Resistivity [10^{-6} Ω.m]	4.3	4.7	17.0	3.0	4.6
d_{av}[b] [µm]	0.25	0.30	0.37	0.15	0.39
d_{50}[b] [µm]	0.11	0.17	0.22	0.12	0.25
d_{90}[b] [µm]	0.54	0.77	0.84	0.33	0.86

[a] crystal size of the secondary phase starting powders;
[b] grain size of the secondary phase

The elastic modulus, E, was obtained by the resonance frequency method (ASTM C 1259-94) on a Grindo-sonic (J.W. Lemmens, Elektronika N.V. Leuven, Belgium). The Vickers hardness, HV_{10}, was measured on a Zwick hardness tester with an indentation weight of 10 kg. The fracture toughness, $K_{IC,10kg}$, was calculated using the formula of Anstis [13], based on crack length measurements of the radial crack pattern produced by Vickers HV_{10} indentations. The electrical resistivity was obtained by the 4-point contact method using a Resistomat Mikroohmmeter (Type 2302, Gernsbach, Germany). Grain size analysis was executed using Imagine-Pro Plus software. The finest grain size distribution of the secondary phase is encountered with grade D, with 50 % of the $TiC_{0.5}N_{0.5}$ grains being smaller than 0.12 µm and 90 % being smaller than 0.33 µm.

Flat specimens of the regarded ZrO_2-based composites were machined and surface finished by grinding or wire-EDM. The grinding operation was executed using JF415DS grinding equipment (Jung, Göppingen, Germany) by means of a diamond abrasive wheel (type MD4075B55, Wendt Boart, Brussels, Belgium) with wheel diameter of 200 mm, average abrasive grain size of 54 µm, wheel speed of 22 m/s, table speed of 12 m/min and cutting depth of 10 µm. Wire-EDM was performed on a ROBOFIL 2000 (Charmilles Technologies, Switzerland) in de-ionized water (dielectric conductivity 11 µS/cm), using CuZn37 wire electrode with diameter 0.25 mm and tensile strength 500 MPa. SEM images in surface view and cross-sectioned view of ZrO_2-WC with wire-EDM surface finish are presented in Fig. 1.

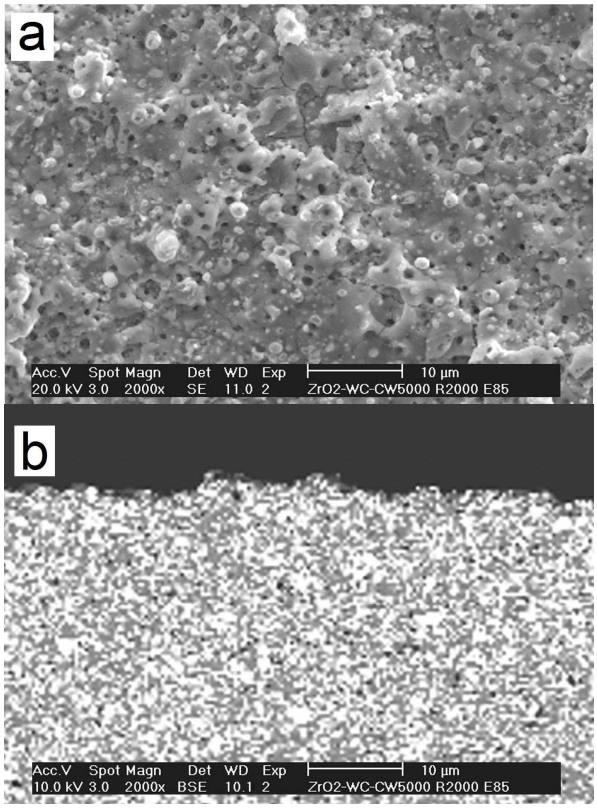

Fig. 1. SEM surface view (a) and cross-sectioned view (b) of wire-EDM'ed ZrO_2-WC grade B

A small amount of heat affected material, containing droplets, craters and micro-cracks, induced by sparking, is visible at the surface, Fig. 1(a). The cross-section view confirms the presence of a thin, re-solidified layer, Fig. 1(b), but does not reveal subsurface cracks nor a clearly defined heat

affected zone, and thus, the microstructure of the composite material beneath the top layer has been maintained. It should be noted that the wire-EDM surface integrity presented in Fig. 1 is representative for the other grades. The R_a and R_t surface roughness for wire-EDM and ground ZrO_2-based composites was obtained according to ISO 4288 and is depicted in Table 2.

Table 2: Surface roughness R_a and R_t [µm] of wire-EDM'ed and ground ZrO_2-based composites

Grade	A	B	C	D	E
Wire-EDM surface finish					
R_a	0.87	1.04	0.70	0.48	0.65
R_t	7.39	8.01	6.37	4.23	5.16
Ground surface finish*					
R_a	0.09	0.04	0.06	0.06	0.18
R_t	0.60	0.35	0.50	0.48	1.42

*Surface roughness measured normal to grinding direction

Wear experiments were performed according to ASTM G133 on a linearly reciprocating-sliding pin-on-flat tribometer TE77 (Phoenix Tribology Ltd, Newbury, England) in unlubricated conditions and in ambient air, i.e., 23±1 °C and 60±1 % relative humidity. Flat specimens of ZrO_2-based composites were kept stationary throughout the tests, whereas WC-6wt%Co cemented carbide counter pins were oscillated with a 10 Hz frequency, a 15 mm stroke length and a concomitant 0.3 m/s average sliding velocity. The pin material displays a compressive strength of 7.2 GPa, a Vickers hardness HV_{10} of 1913 kg/mm^2, a fracture toughness $K_{IC,10kg}$ of 8.4 MPa m$^{1/2}$ and an E-modulus of 609 GPa. The pins were machined by the supplier. The pin tip was a hemisphere with diameter 8.08 mm and a surface roughness R_a and R_t of 0.35 µm and 2.68 µm respectively. The total sliding distance in each test was 10 km. Normal contact forces of 15, 25 and 35 N were imposed, commensurate with initial mean Hertzian contact pressures between 1.30 and 1.91 GPa for the regarded ZrO_2-composite vs. WC-6wt%Co combinations. The applied normal force (F_N) and the concomitant tangential frictional force (F_T) were measured continuously. The F_T/F_N forces ratio is defined as the coefficient of friction (μ), which can be differentiated in a static, i.e., μ_s, and a dynamic, i.e., μ_d, component. Vertical displacement (Δd_p) curves resulting from the combined wear of WC-6wt%Co pins penetrating the zirconia-based counter samples were recorded using an inductive displacement transducer. Each wear test was repeated 3 times and averages values and deviations were calculated to obtain representative friction and wear data. For each wear experiment, a new pin was used. Prior to wear testing, pin and flat samples were cleaned ultrasonically for 0.25 h at 50 °C in distilled water with a detergent solution (2% Tickopur R33, DR-H-STAMM GmbH Chemische Fabrik, Berlin, Germany), subsequently immersed in acetone, dried in air and rinsed with cold distilled water to remove possible traces of alcohol from the specimens.

After wear testing, the worn surfaces were cleared by pressurized air. Post-mortem wear was quantified using topographical scanning equipment (Hommel Somicronic® EMS Surfascan 3D, type SM3, stylus type ST305, St.-André-de-Corcy, France). Wear scars and debris were analyzed by scanning electron microscopy (SEM, XL-30 FEG, FEI, The Netherlands), equipped with an energy dispersive X-ray spectroscopy system (EDS). X-ray diffraction (XRD) measurements were performed on a θ-θ diffractometer (3003-TT, Seifert, Ahrensburg, Germany) using Cu-Kα radiation (40 kV, 30 mA).

3. RESULTS

3.1. Friction coefficient

Average friction coefficient curves for WC-6wt%Co pins in oscillating sliding contact with ZrO_2-based composite flats are plotted as function of sliding distance (s) in Fig. 2. Error bars indicating the extent of the variations are excluded in order to improve the readability of the graphs. Compared to the static friction coefficient, the dynamic friction coefficient is discerned to display lower values but varies similarly as function of

sliding distance: abruptly increasing during the first meters of sliding, subsequently declining and increasing again. After running-in, the fluctuations in friction coefficient are considerably smaller, indicating that an equilibrium situation is being reached. Beyond a sliding distance of 4 km, the variations in friction coefficient become marginal.

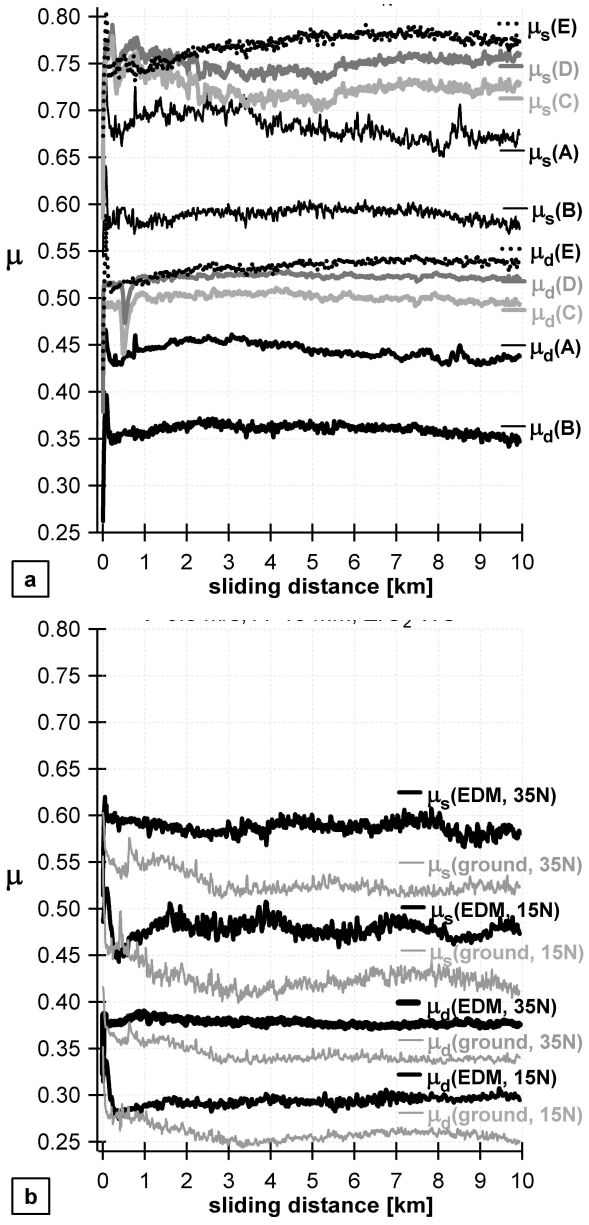

Fig. 2. Friction coefficient (μ_s, μ_d) for WC-6wt%Co pins sliding at 0.3 m/s against (a) 5 wire-EDM'ed ZrO_2-based grades using 25 N contact force or (b) ZrO_2-WC grade B with wire-EDM and ground surface finish using 15 N and 35 N contact force

Within the full sliding distance range, the static and dynamic friction coefficient was measured to be between 0.56 and 0.80 and between 0.34 and 0.54 respectively. The temporary drop down followed by a steep increase, as observed for both ZrO_2-TiCN grades in Fig. 2(a) could be related to changes in the sliding contact surface due to removal of the wire-EDM induced heat affected material. In full agreement with literature data on friction and wear behaviour of alumina-based and zirconia-based composites [3] and previous investigation described in [12], the effect of the secondary phase on friction coefficient is quite significant. The lowest friction level was recorded for ZrO_2-WC grade B vs. WC-6wt.%Co sliding combinations, whereas ZrO_2-TiN grade E yielded the highest friction coefficient.

The effect of surface finishing and load conditions on friction behavior of ZrO_2-WC/WC-6wt%Co combinations is examined in Fig. 2(b). Under the imposed normal contact forces, the static and dynamic friction coefficient was measured to be in the 0.41–0.62 and 0.25–0.39 range, respectively. Compared to the frictional characteristics exhibited by ground ZrO_2-WC composites a higher friction level is encountered with identical wire-EDM'ed material. The coefficient of friction is also higher when normal contact loads were heavier. It is worth noting that similar trends were observed for the other ZrO_2-based composites. Furthermore, the relative difference in friction level between ground and wire-EDM'ed samples was discerned to slightly diminish at higher contact loads and with increasing sliding distance.

3.2. Wear characteristics

Average wear curves (Δd_p) during reciprocating sliding of wire-EDM'ed and ground ZrO_2-based composite flats vs. WC-6wt%Co pins are plotted against sliding distance in Fig. 3. In all cases, the penetration depth first increases abruptly, owing to quickly growing contact surface area, and subsequently increases more slowly, varying almost linearly with sliding distance, presuming that the wear process reaches an equilibrium.

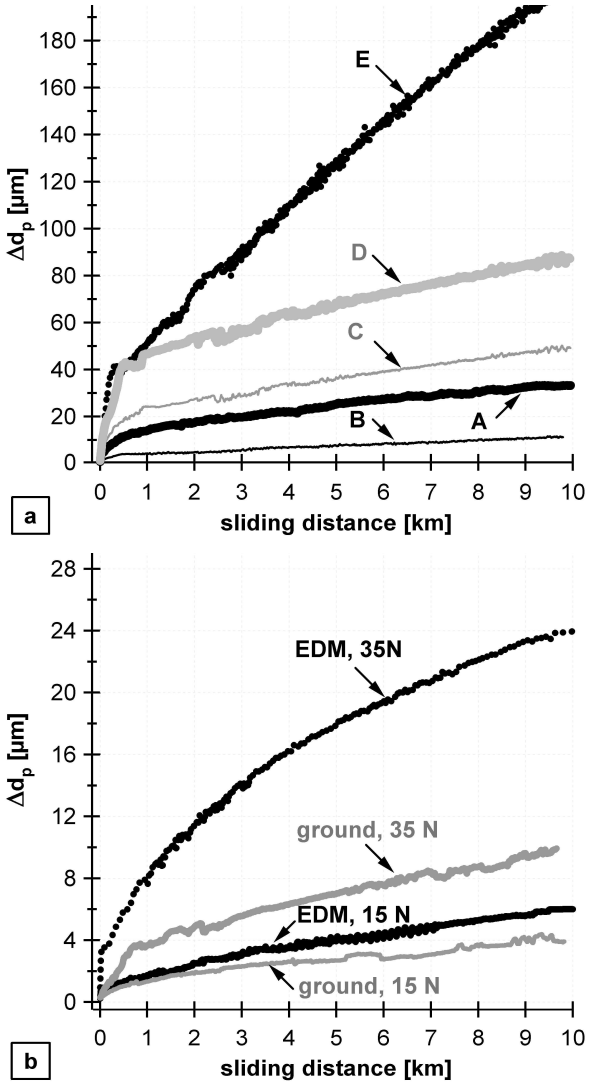

Fig. 3. Penetration depth (Δd_p) for ZrO_2-based composites vs. WC-6wt%Co pins sliding at 0.3 m/s under (a) 25 N contact force for wire-EDM'ed ZrO_2-based grades or (b) 15 N and 35 N contact force for wire-EDM'ed and ground ZrO_2-WC grade B

The strong influence of the secondary phase of the zirconia composites on friction characteristics, Fig. 2(a), is reflected in the corresponding wear data, Fig. 3(a). In the full wear path range, the largest wear depth is recorded for ZrO_2-TiN, whereas the ZrO_2-WC grade B displays the lowest wear level. The impact of wire-EDM on the wear curves is quite pronounced, Fig. 3(b). Consistently with the friction coefficient curves in Fig. 2(b) and in agreement with previous research on tribological characteristics of wire-EDM'ed and polished ZrO_2-TiN composites [11], the penetration depth of the investigated sliding pairs was larger for wire-EDM'ed samples compared to equivalent ground material, especially during initial sliding. Moreover, the wear levels are found to be higher when a heavier normal contact load is imposed. It should be noted that the trends observed in Fig. 3(b) were also found for the other ZrO_2-based composites.

Results of post-mortem quantified wear track volumes for ZrO_2-based composites are depicted in Fig. 4, demonstrating how the wear properties are affected by surface finishing operation, the nature of the secondary phase and the imposed normal contact force. Wear volumes after 10 km sliding are noticed to vary over more than 3 orders of magnitude, i.e., between 6.8×10^{-3} and 9.8 mm^3.

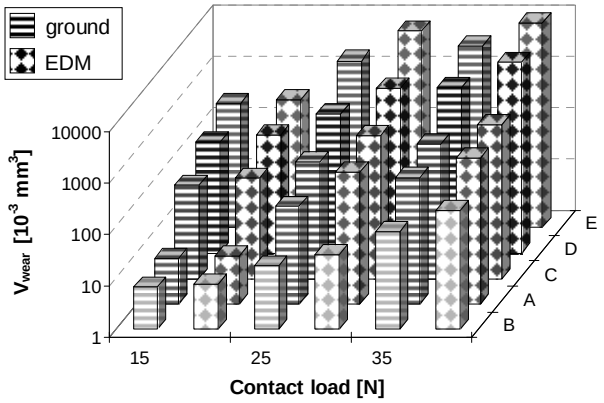

Fig. 4. Post-mortem volumetric wear as function of contact load and surface finish for ZrO_2-based grades slid against WC-6wt%Co pins for 10 km at 0.3 m/s

Under equal test parameters of wear path, surface finish and contact load, the lowest wear volumes were recorded for ZrO_2-WC grade B, whereas the largest values occurred for ZrO_2-TiN specimens, in full agreement with the results of Fig. 3. The sequence of ZrO_2-WC, ZrO_2-TiCN and ZrO_2-TiN for relative wear quantification ranking was also found in previous investigation [12]. Similarly, the highest volumetric wear is encountered with wire-EDM'ed surfaces compared to equivalent ground ZrO_2-based composites. Furthermore, for each grade, the largest wear level was encountered when the heaviest contact loads were imposed.

3.3. Flexural strength

The effect of surface finish operations on friction and wear was also reflected in the flexural strength. This is demonstrated in Fig. 5, which compares the results of three-point bending tests on ZrO_2-based composites with wire-EDM and ground surface finish. The flexure experiments were carried out at room temperature. The span width was 20 mm with a crosshead displacement of 0.1 mm/min. The ZrO_2-based composite samples (45.0 mm × 4.3 mm × 1.44 mm) were machined out of a hot pressed disc and subsequently surface finished by wire-EDM on a ROBOFIL 2000 (Charmilles Technologies, Geneva, Switzerland) or by a diamond grinding wheel (Wendt Boart, type MD4075B55, Brussels, Belgium). The flexural strength is substantially lower after wire-EDM compared to grinding, Fig. 5. The strength degradation due to wire-EDM is most striking for ZrO_2-WC grade A.

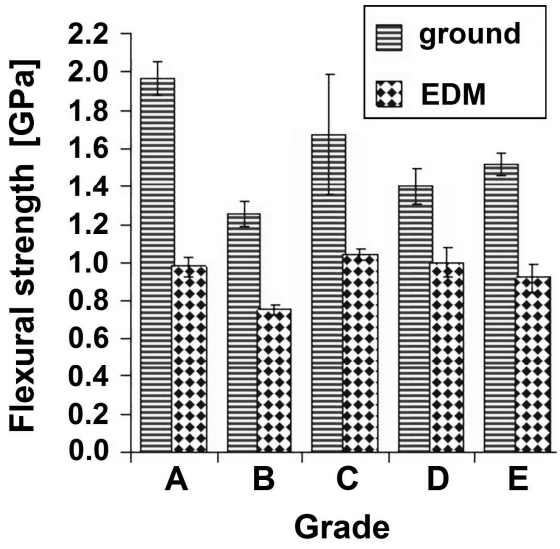

Fig. 5. 3-point bending strength of wire-EDM'ed and ground ZrO_2-based grades

3.4. Wear surface observation

Optical inspection of the wear track surface of ZrO_2-based composites after sliding against WC-6wt%Co for 10 km at 10 Hz oscillating frequency under various contact loads revealed the presence of wear debris, mainly located in the outer extensions of the sliding contact interface, but occasionally also inside, along and adjacent to the complete wear tracks. The aspect of the wear surface was smoother compared to the original wire-EDM or ground surface finishes. This finding implies that the original surface roughness peaks, particularly in the case of wire-EDM'ed ZrO_2-based composites, are polished off during sliding contact. The smooth aspect of the wear surfaces could also be the result of (small amounts of) adhered wear debris originating from WC-6wt%Co pin and ZrO_2-based composite. This phenomenon was confirmed by profilometric surface scanning on ZrO_2-based composites before and after wear testing. For example, R_a- and R_t-values of 0.02 µm and 0.28 µm respectively were derived in the wear track of the ZrO_2-TiCN grade C after 10 km of sliding, which is quite below the R_a- and R_t-values characterizing the original wire-EDM surface finish, Table 2.

SEM observation as well as EDX and XRD analysis on wear debris originating from ZrO_2-TiCN is presented in Fig. 6. No phases could be differentiated in the debris, Fig. 6(a), indicating that the original ZrO_2 and TiCN phases are integrated in the debris material. EDX analysis on the wear debris collected from a tested ZrO_2-TiCN grade C reveals the elements Zr, Ti, Al, O, W and Co in its chemical composition, as shown in Fig. 6(b). It should be clear that Co originates from the WC-6wt%Co pin material. The corresponding XRD spectrum reveals the presence of a crystalline $ZrTiO_4$ reaction product in the wear debris, Fig. 6(c). The size of the debris particles is in the nanometer range. The Si peak in the X-ray diffraction pattern is owing to the fact that the debris was collected on a silicon wafer.

Fig. 7 presents SEM images of worn surface in the central wear tracks of wire-EDM'ed ZrO_2-WC grade B slid against WC-6wt%Co for 10 km at 0.3 m/s under 15 N and 35 N. The effect of polishing as a result of the sliding contact with the pin is demonstrated in Figs. 6(a) and 6(c), in which the wear track can clearly be distinguished from the original wire-EDM surface.

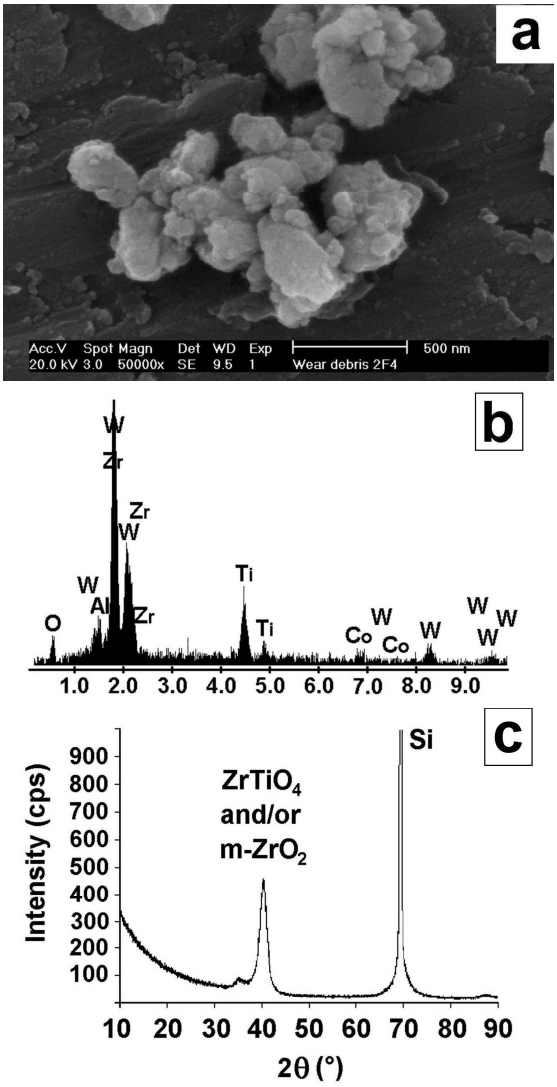

Fig. 6. Analysis by SEM (a), EDX (b) and XRD (c) on wear debris derived from wire-EDM'ed ZrO_2–TiCN grade C after sliding against WC–6wt%Co at 0.3 m/s under 35 N normal contact force

Comparing Figs. 6(a) and 6(c) reveals that the wear track resulting from a 35 N wear test displays a higher width compared to the equivalent 15 N wear test. Fig. 6(b) shows that, when a contact load of 15 N was applied, the microstructure in the wear track mainly corresponds to that of the pristine material. Furthermore, small amounts of wear debris and wear debris layer can be observed. For sliding wear tests with a 35 N contact load, however, the wear track is covered with larger areas of wear debris layer, Fig. 6(d). Micro-cracks are observed in the wear debris layer all along the wear track, whereas the debris layer tends to delaminate. It is worth noting that similar observations were made for the wire-EDM'ed ZrO_2-WC grade A.

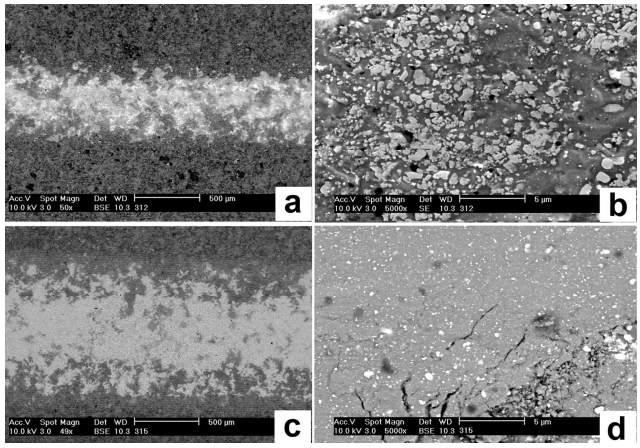

Fig. 7. SEM micrographs at different magnifications of the wear track of wire-EDM'ed ZrO_2-WC grade B after sliding for 10 km at 0.3 m/s against WC-6wt%Co pins under a contact load of 15 N (a, b) or 35 N (c, d)

Wear surface observations of the zirconia based composites as function of contact load, chemical composition and surface finish condition are summarized in Table 3. The formation of a continuous debris layer in the wear track was only observed when contact loads of 35 N were imposed. The ZrO_2-TiCN composite turns out to be less prone to the formation of a continuous debris layer compared to the ZrO_2-WC and ZrO_2-TiN composites. When testing at 15 or 25 N, the microstructure in the wear track appeared mainly like the original base material.

Table 3: Correlation between surface state[a], surface finish and contact load for ZrO_2-based composites slid for 10 km at 0.3 m/s against WC-6wt%Co

Grade	A	B	C	D	E
Wire-EDM surface finish					
Load: 15 N	C	C	C	C	C
Load: 25 N	C	C	C	I	I
Load: 35 N	D	D	I	D	D
Ground surface finish					
Load: 15 N	C	C	C	C	C
Load: 25 N	C	C	C	C	C
Load: 35 N	I	I	I	I	D

[a] C: clean; D: debris layer formation; I: debris layer initiation

4. CONCLUSIONS

Reciprocating wear testing of ZrO_2-WC, ZrO_2-TiCN and ZrO_2-TiN composites with different surface finishes in dry sliding contact with WC-6wt%Co revealed that wire-EDM, compared to grinding, involves increased friction and higher wear level due to a more pronounced occurrence of wear mechanisms, i.e., polishing, (micro) abrasion, grain cracking, grain removal and the formation, compaction, adhesion, spalling and delamination of wear debris (layer). The inferior wear resistance for wire-EDM compared to grinding was also reflected in lower flexural strength. Amongst the ZrO_2-based composites the lowest friction coefficient and wear volume were encountered with ZrO_2-WC grades, whereas ZrO_2-TiN displayed the highest friction and wear. Wear resistance of ZrO_2-TiCN grades was in-between that of ZrO_2-WC and ZrO_2-TiN.

5. ACKNOWLEDGEMENTS

This research was supported by the Flemish Institute for promotion of Innovation by Science and Technology in industry (IWT, Grant No. GBOU-IWT-010071-SPARK) and by the Fund for Scientific Research Flanders (FWO, Grant No. G.0539.08). Investigation was performed within a cooperative effort among Ghent University (UGent) and Catholic University of Leuven (K.U.Leuven). The authors wish to thank CERATIZIT for supplying the hardmetal pins.

6. REFERENCES

[1] Lee Soo W, Hsu SM, Shen MC. Ceramic wear maps: zirconia. J Am Ceram Soc 1993;76(8):1937-1947

[2] Yang C-CT, Wei W-CJ. Effects of material properties and testing parameters on wear properties of fine-grain zirconia TZP. Wear 2000;242(1):97–104

[3] He YJ et al. Effects of a second phase on the tribological properties of Al_2O_3 and ZrO_2 ceramics. Wear 1997;210(1-2):178-187

[4] Anné G et al. Hard, tough and strong ZrO_2-WC composites from nanosized powders. J Eur Ceram Soc 2005;25(1):55-63

[5] Jiang D et al. Development and characterization of ZrO_2-$TiC_{0.5}N_{0.5}$ nanocomposites. Proc 9th Conf & Exhib Eur Ceram Soc, 2005, Slovenia; 19–23

[6] Salehi S, Van der Biest O, Vleugels J. Electrically conductive ZrO_2-TiN composites. J Eur Ceram Soc 2006;26(15):3173-3179

[7] Zum Gahr K-H. Wear by hard particles. Tribology International 1998;31(10):587-596

[8] Kozak J, Rajurkar KP, Chandarana N. Machining of low electrical conductive materials by wire electrical discharge machining (WEDM). J Mater Process Tech 2004;149(1-3):266-271

[9] Lauwers B et al. Investigation of material removal mechanisms in EDM of composite ceramic materials. J Mater Process Tech 2004;149(1-3):347-352

[10] Bonny K et al. Influence of secondary electro-conductive phases on the electrical discharge machinability and frictional behavior of ZrO_2-based ceramic composites. J Mater Process Tech 2008;208(1-3):423-430

[11] Bonny K et al. Influence of electrical discharge machining on tribological behavior of ZrO_2-TiN composites. Wear 2009;265(11-12):1884-1892

[12] Bonny K et al. Reciprocating sliding friction and wear behavior of Electrical Discharge Machined Zirconia-based Composites against WC-Co Cemented Carbide. Int J Refract Met Hard Mater 2009;27(2):449-457

[13] Anstis GR et al. A critical evaluation of indentation techniques for measuring fracture toughness: I, direct crack measurements. J Eur Ceram Soc 1981;64(9):533–538